

UNCLASSIFIED

Defense Technical Information Center
Compilation Part Notice

ADP012253

TITLE: Superconductivity of Embedded Lead Nanoparticles in Metallic and Aamorphous Matrices

DISTRIBUTION: Approved for public release, distribution unlimited

This paper is part of the following report:

TITLE: Nanophase and Nanocomposite Materials IV held in Boston, Massachusetts on November 26-29, 2001

To order the complete compilation report, use: ADA401575

The component part is provided here to allow users access to individually authored sections of proceedings, annals, symposia, etc. However, the component should be considered within the context of the overall compilation report and not as a stand-alone technical report.

The following component part numbers comprise the compilation report:

ADP012174 thru ADP012259

UNCLASSIFIED

Superconductivity of embedded lead nano particles in metallic and amorphous matrices

K. Chattopadhyay^a, V. Bhattacharya^a and A. P. Tsai^b

^aIndian Institute of Science, Bangalore-560 012, India

^bNational Research Institute for Metals, Tsukuba 305-0047, Japan

ABSTRACT

Nanodispersed lead in metallic and amorphous matrices was synthesized by rapid solidification processing. The optimum microstructure was tailored to avoid percolation of the particles. With these embedded particles it is possible to study quantitatively the effect of size on the superconducting transition temperature by carrying out quantitative microstructural characterization and magnetic measurements. Our results suggest the role of the matrices in enhancement or depression of superconducting transition temperature of lead. The origin of this difference in behavior with respect to different matrices and sizes is discussed.

INTRODUCTION

The early observations on the importance of normal-superconductor junctions were made in 1930 [1]. Since then a large body of literature are available on the subject. Intensive theoretical and experimental investigations were carried out in the sixties and seventies on granular superconductors and thin films [2,3,4]. Recently, there is a resurgence of interest due to the increasing interest in nanoscience and technology which demands understanding the behaviour of small particles [5-9]. Rapid solidification technique has been extensively used to synthesize nanoembedded particles of immiscible alloy [10]. We have successfully synthesized nanosized Pb dispersed in different matrices using this technique. In the present paper, we report the superconductive behaviour of these nanosized Pb particles embedded in Al and Al-based metallic glass matrices.

EXPERIMENTAL PROCEDURE

Nanoembedded lead in aluminium and amorphous glassy matrix was synthesized via melt spinning using 99.999%Al, Cu, V and 99.99%Pb. An optimum composition and quenching rate was chosen in order to obtain a well-dispersed microstructure. Lead is insoluble in aluminium, and in all the three elements constituting the $Al_{75}Cu_{15}V_{10}$ matrix both in the liquid state and the solid state. The processing resulted in an aluminium matrix with nanodispersions of lead, and a metallic glass matrix with nano lead dispersions. Preliminary phase identification of the samples were carried out by X-ray diffraction (JEOL model JDX 8030) using Cu K_{α} radiation. Microstructural characterisation was done using a JEOL 2000 FX-II Transmission Electron Microscope (TEM) and HREM. The size distributions of particles were carried out using a

Sigma scan Pro commercial software. Magnetic measurements were carried out in a SQUID magnetometer in standard configuration. The magnetization tests were conducted under identical conditions in zero field-cooled state in order to avoid the interference of macroscopic persistent screening currents flowing in the sample. Typical fields of 200c & 1000c were chosen for measurements.

RESULTS

The composition of Pb in Al was 6.5wt% and in $\text{Al}_{75}\text{Cu}_{15}\text{V}_{10}$ was 20wt%. The detailed results of the glassy matrix has been given elsewhere [9]. Fig. 1(a) shows an electron micrograph of dispersed Pb in aluminium matrix and Fig. 1(b) shows the corresponding size distribution plot. Fig 1(c) shows the selected electron diffraction pattern from both the dispersed Pb phase and matrix confirming the cube on cube orientation relationship of Pb with Al. There exists a significant difference of lattice parameters of the two fcc cubic phases. Pb has a lattice parameter of 0.47nm while the corresponding value for Al is 0.401nm. However, no strain field could be visible around Pb particles in Al matrix. Fig 2 shows the size distribution of lead in glassy matrix obtained from high-resolution images. The Pb particle in this case is randomly oriented.

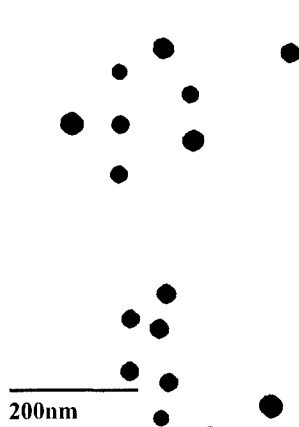


Figure 1(a) Electron micrograph showing nano dispersed Pb in Al

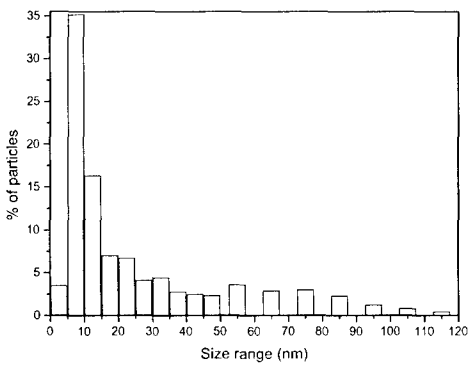


Figure 1(b) Size distribution showing Pb dispersoids in Al

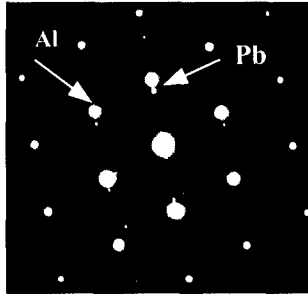


Figure 1(c) SADP showing Al and Pb reflections possessing cube on cube O.R

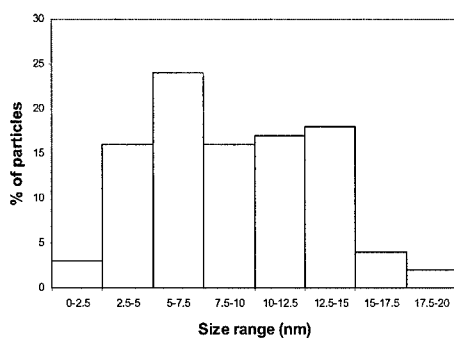


Figure.2 Size distribution of Pb in glassy matrix

The magnetization vs temperature plots for both Pb embedded in Al-Cu-V metallic glass and Al matrices are shown in Fig. 3 and Fig.4 respectively measured at a field of 20 Oe. For comparison, measurements are also made on bulk samples of lead (see fig.3).

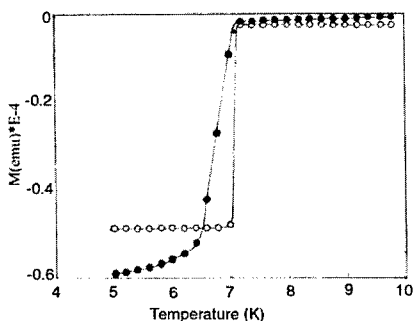


Figure 3 Magnetization with temperature for $\text{Al}_{75}\text{Cu}_{15}\text{V}_{10}$ -20wt%Pb measured with a field of 20Oe. Hollow circles represent data of bulk Pb and solid circles represent Pb in glassy matrix

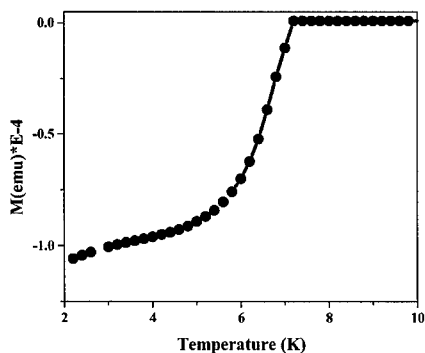


Figure 4 Magnetization vs temperature for Al-6.5wt% Pb measured with a field of 20Oe

The transition in the bulk lead sample is sharp and the entire sample becomes superconducting at $T_c \sim 7.2\text{K}$.

The transition temperature of the nanodispersed lead in both the aluminium and glassy matrices occurs over a range of temperature and the magnetization curve shows a sigmoidal behaviour. Fig.5 shows a typical cumulative size distribution plot obtained from the measurement of ~ 5000 particles for Pb dispersed in Al matrix. The optimum numbers of particles for measurements

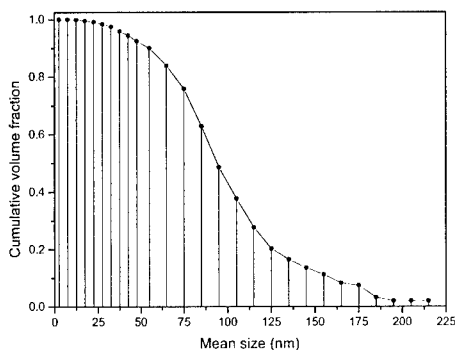


Figure 5 Cumulative volume fraction starting from the larger particle which becomes superconducting first

were determined by ensuring that the nature of the cumulative plot does not change with increase in particle number. Assuming a spherical particle, it is possible to convert this to volume distribution of each size. The depression of the superconducting transition temperature occurs with decreasing particle size. Since, magnetization is expressed per unit volume, it is possible to map the two curves and obtain a relation between transition temperature and size. Fig.6 shows such a curve for Pb distributed in Al matrix. Fig.7 shows a comparative plot of Pb in Al and glassy $\text{Al}_{75}\text{Cu}_{15}\text{V}_{10}$ matrix.

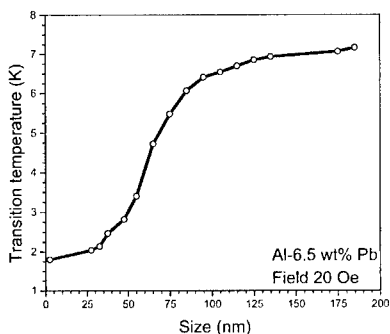


Figure 6 Computed temperature vs size plot for Pb in Al matrix

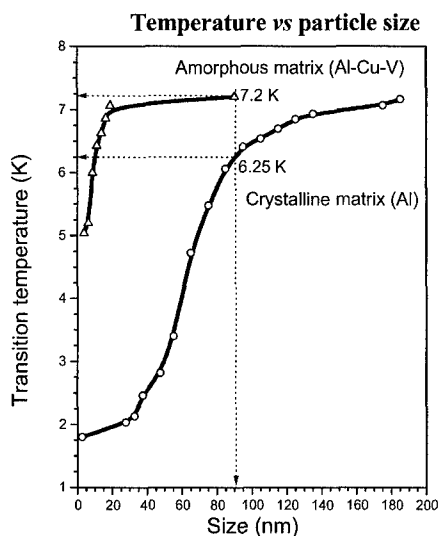


Figure 7 Comparative transition temperature Vs size plot for Pb dispersed in Al and Al-Cu-V glassy matrix

DISCUSSION

From our experiments, it is clear that the critical temperature of superconducting transition scales with size in a non-linear fashion. Compared to our earlier work with glassy matrix [9], the depression sets in much earlier when the particles are embedded in crystalline aluminium matrix. The effect of interface on superconductivity was studied earlier in the context of thin films [2,3,4]. These studies were conducted on evaporated layers of lead on copper and aluminium, and the layer packets produced by quench condensation at a substrate at 10K show a similar trend in transition temperature Vs thickness plot. The transition temperature of the lead layer falls rapidly as a function of thickness and drops rapidly when $D_{Pb} < 50\text{nm}$. From their plot, it is possible to extrapolate to a critical thickness of 10nm, when transition temperature approaches 1K. These results clearly revealed the depression of critical temperature as a function of film thickness. The essential difference between our situation and thin films lies in the nature of the confinement. In our case, the number of electrons in the system decreases significantly leading to discreteness of the energy levels [11]. Further, since the sizes of our particles in most cases are smaller than the coherence length in all directions, it can be considered as a zero dimensional superconductor. In such a case, the nature of the lattice of the embedding matrix is expected to play a significant role. This is clearly highlighted in the comparative plot in Fig.7. The depression in glassy matrix sets in at much smaller size range compared to the crystalline aluminium matrix. In principle, one should be able to correlate this difference with the penetration of Cooper pairs in the two normal embedding matrices. We are unable to estimate this at the present moment. We also note that T_c for Pb particles having size equal to bulk coherence length is depressed for crystalline Al matrix whereas those in the glassy matrix at this size show bulk behaviour. Using the theory of superconductor of Anderson [12], Strongin et al [13] suggested the following expression for the relation between superconducting transition and energy level spacings for spherical granules:

$$\ln (T_c/T_{c0}) = \sum [2/(2m+1)] \times \{ \tanh [(\pi/2)((2m+1)2\pi k_B T_c/\epsilon)] - 1 \}$$

Here, T_{c0} and T_c is the transition temperature for the bulk and the small particles and ϵ is the energy level spacing. According to this, for Pb, the superconductivity can be sustained up to a size of 2.2nm. In that case, both the curves in Fig. 7 should cut the y-axis at the same value. Within the experimental accuracy of our measurements, the trends of our curves seem to be different. This raises the need for more accurate experiments at small sizes. From the comparative plot it is shown that for the same size range the depression in T_c is much more for a crystalline matrix compared to the glassy matrix. Clearly, exchange of Cooper pairs and normal electrons across the interface is limited in glassy matrix compared to crystalline matrix. The data in both cases indicate a sigmoidal curve characteristic of Boltzmann distribution. It can be pointed out that the analysis of this behaviour is not possible with mean field BCS theory because of the finite number of electrons in each particle. This aspect has recently been discussed by Braun and Delft [14]. The analysis is not amenable at this stage to quantitative comparison with our experiments.

CONCLUSION

We have established the size dependence of T_c for Pb particles embedded in Al matrix. We have compared this result with that obtained for a metallic glass matrix. The results suggest a distinct difference in the behaviour of depression and indicate an important influence of the particle matrix interface in determining the depression of T_c .

ACKNOWLEDGEMENT

The authors acknowledge STA, Japan and Department of Science and Technology, India for their financial support.

REFERENCES

- [1] Burton, E.F, J. O. Wilhelm and A.D. Misener: Trans. Roy. Soc. Canada. **29**(III), 5 (1934)
- [2] P. Hilsch: Z. Phys. **167**, 511 (1962)
- [3] G. Bergmann: Z. Phys, **187**,395 (1965)
- [4] G.V. Minnigerode : Z. Phys. **192**, 379, (1966)
- [5] B. Muhlschegel, D. J.Scalapino & R. Dutta, Phys.Rev.B. **6**, 5 (1972)
- [6] K.A. Matven &A.I. Larkin, Phys. Rev. Letters, **78**, 19, 3749 (1997)
- [7] F. Braun, J. v. Delft, D.C. Ralph & M. Tinkan, Phys. Rev. Letters, **79**, 5, 921 (1997)
- [8] F. Braun& J. v. Delft, Phys Rev B, **59**,14,9527 (1999)
- [9] A.P. Tsai, N. Chandrasekhar and K. Chattopadhyay, App. Phys. Lett. **75**, 11, 1527 (1999)
- [10] K. Chattopadhyay, Mat. Sci. and Engg A, **226**, 1012 (1997)
- [11] R. Kubo, J. Phys. Soc. Jpn **17**, 975 (1962)
- [12] P. W. Anderson, J. Phys. Chem. Solids **11**, 26 (1959)
- [13] M. Strongin, R. S. Thompson, O. F. Krammerer, and J. E. Crow, Phys. Rev. B **1**, 1078 (1970)
- [14] F. Braun and J. v. Heft, Phys. Rev. letters, **81**, 21, 4721(1998)